

Drug release from PLGA microparticles can be slowed down by a surrounding hydrogel

L.A. Lefol^a, P. Bawuah^b, J.A. Zeitler^b, J. Verin^a, F. Danede^c, J.F. Willart^c, F. Siepmann^a, J. Siepmann^{a,*}

^a Univ. Lille, Inserm, CHU Lille, U1008, Lille F-59000, France

^b Univ. Cambridge, Department of Chemical Engineering and Biotechnology, Cambridge CB3 0AS, UK

^c Univ. Lille, USTL UMET UMR CNRS 8207, Villeneuve d'Ascq F-59650, France

ARTICLE INFO

Keywords:

PLGA
Microparticles
Drug release mechanism
Experimental setup
Swelling
Agarose gel

ABSTRACT

This study aimed to evaluate and better understand the potential impact that a layer of surrounding hydrogel (mimicking living tissue) can have on the drug release from PLGA microparticles. Ibuprofen-loaded microparticles were prepared with an emulsion solvent extraction/evaporation method. The drug loading was about 48%. The surface of the microparticles appeared initially smooth and non-porous. In contrast, the internal microstructure of the particles exhibited a continuous network of tiny pores. Ibuprofen release from *single* microparticles was measured into agarose gels and well-agitated phosphate buffer pH 7.4. Optical microscopy, scanning electron microscopy, differential scanning calorimetry, X-ray powder diffraction, and X-ray μ CT imaging were used to characterize the microparticles before and after exposure to the release media. Importantly, ibuprofen release was much slower in the presence of a surrounding agarose gel, e.g., the complete release took two weeks vs. a few days in well agitated phosphate buffer. This can probably be attributed to the fact that the hydrogel sterically hinders substantial system swelling and, thus, slows down the related increase in drug mobility. In addition, *in this particular case*, the convective flow in agitated bulk fluid likely damages the thin PLGA layer at the microparticles' surface, giving the outer aqueous phase more rapid access to the inner continuous pore network: Upon contact with water, the drug dissolves and rapidly diffuses out through a continuous network of water-filled channels. Without direct surface access, most of the drug "has to wait" for the onset of substantial system swelling to be released.

1. Introduction

Poly(lactic-co-glycolic acid) (PLGA) is frequently used as a polymeric matrix former in parenteral controlled drug delivery systems, in particular for microparticles and implants (Dorta et al., 2002; Hirankumar and Steven, 2012; Feng et al., 2014; Lagreca et al., 2020; Mirzaeei et al., 2021). Key advantages include its biocompatibility and biodegradability (Anderson and Shive, 2012). Several drug products based on PLGA have been approved by the FDA and/or the EMA, including, for instance, Lupron Depot, Ozurdex, Risperidal Consta, Atridox, and Zoladex Depot (Zhong et al., 2018). Importantly, different manufacturing processes can be used to prepare PLGA-based drug products, such as 3D printing (Guo et al., 2019; F. Sun et al., 2022), hot melt extrusion (Ghalanbor et al., 2012; Bassand et al., 2022a), direct compression (Takahashi et al., 2004; Yelles et al., 2017), emulsion

solvent-extraction/evaporation methods (Donnell and McGinity, 1997; Pean et al., 1998; Amoyav and Benny, 2019; Park et al., 2021) and spray-drying (Wan and Yang, 2016; Arpagaus, 2019). Desired drug release rates can be adjusted by varying the formulation and processing parameters, for example, the PLGA chemistry and system size (Berkland et al., 2002; Klose et al., 2006; Qi et al., 2019; Benhabbour et al., 2019; Wang et al., 2020). Compared to *implants*, microparticles offer the advantage of a less invasive administration.

Despite the tremendous practical importance of PLGA-based drug delivery systems, the underlying mass transport mechanisms are often not fully understood (Shah et al., 1992; Fredenberg et al., 2011; Gasmi et al., 2016). This complicates drug product optimization because unexpected tendencies can be observed when varying a formulation parameter. One of the reasons for the frequently encountered limited understanding of how drug release is controlled from such an advanced

* Corresponding author at: College of Pharmacy, INSERM U1008, University of Lille, 3, rue du Professeur Laguesse, Lille 59006, France.

E-mail address: juergen.siepmann@univ-lille.fr (J. Siepmann).

<https://doi.org/10.1016/j.ijpx.2023.100220>

Received 24 July 2023; Received in revised form 23 November 2023; Accepted 25 November 2023

Available online 28 November 2023

2590-1567/© 2023 The Authors. Published by Elsevier B.V. This is an open access article under the CC BY-NC-ND license (<http://creativecommons.org/licenses/by-nc-nd/4.0/>).

delivery system, is the complexity of the involved physico-chemical phenomena. The latter include, for instance, penetration of water into the system, drug dissolution, polymer degradation, polymer swelling (Gasmi et al., 2015a, 2015b; Tamani et al., 2019; Bode et al., 2019), drug diffusion through water-filled channels and/or a continuous PLGA phase, osmotic effects (Brunner et al., 1999), the creation of local acidic microenvironments within the dosage form (Fu et al., 2000; Liu et al., 2008), autocatalytic effects (Siepmann et al., 2005; Ford et al., 2013), drug precipitation (Mirzaeei et al., 2021), drug-polymer interactions, plasticizing effects of water (Blasi et al., 2005) and/or of the drug (Blasi et al., 2007), the creation and closure of pores (Kim et al., 2006; Kang and Schwendeman, 2007) as well as limited drug solubility effects within and outside of the dosage form (Gasmi et al., 2016), to mention just a few. It has to be pointed out that the *relative* importance of these phenomena can substantially differ from system to system. For example, drug release might already be complete before substantial system swelling commences. Various formulation and processing parameters can fundamentally affect the conditions for drug release and, thus, the *dominant* release mechanism(s), for instance, the composition of the device (e.g., drug and PLGA content, presence of further excipients), type of drug (e.g., molecular weight, solubility, acidity), geometry and dimensions of the dosage form, inner and outer system morphology (e.g., porosity).

When observing drug release from PLGA-based drug delivery systems *in vitro*, it should not be forgotten that the provided experimental conditions might artificially impact at least some of the involved physico-chemical processes. For example, it has been reported that a surrounding hydrogel can mechanically hinder the swelling of PLGA-based *implants* and slow down drug release (Kožák et al., 2021; Bas-sand et al., 2022b). The hydrogel is intended to mimic living tissue, which surrounds the dosage form *in vivo* in the patient (Ye et al., 2012; Sun et al., 2017; Li et al., 2021). This mechanical resistance of the environment is not simulated when studying drug release with the frequently used standard setup, where the particles are simply exposed to well-agitated bulk fluid. Consequently, the drug release kinetics observed *in vitro* might not predict drug release *in vivo*. However, it is yet unclear if the presence of a surrounding hydrogel might also impact drug release from PLGA-based *microparticles*. Since the dimensions are different, the importance of the effects may differ.

This study aimed to investigate whether an agarose gel surrounding PLGA-based *microparticles* can have a similar effect on drug release as this is the case with PLGA-based *implants*. Importantly, drug release was measured from *single* microparticles. Ensembles of (e.g., thousands of particles) are administered in practice. And in most cases, drug release is monitored from such *ensembles* of microparticles. However, the observed drug release rates are the sum of the individual release rates from all microparticles. It must be noted that considerable variability in the release kinetics from individual microparticles can generally be expected (even from the same batch) (Tamani et al., 2019, 2021). This is because each microparticle is different, e.g., it has a specific size, drug loading, and inner structure (including drug distribution when drug particles are dispersed within a polymeric matrix). When elucidating the drug release mechanisms from such *multiple* unit dosage forms, it is crucial to investigate the behavior also of the *single* microparticles. Ibuprofen-loaded PLGA microparticles were prepared using an emulsion solvent extraction/evaporation technique. Drug release from *single* microparticles was monitored in agarose gels and well-agitated phosphate buffer pH 7.4 at 37 °C. Optical and scanning electron microscopy, X-ray micro computed tomography, X-ray powder diffraction, and differential scanning calorimetry were used to thoroughly characterize the microparticles before and after exposure to the release media.

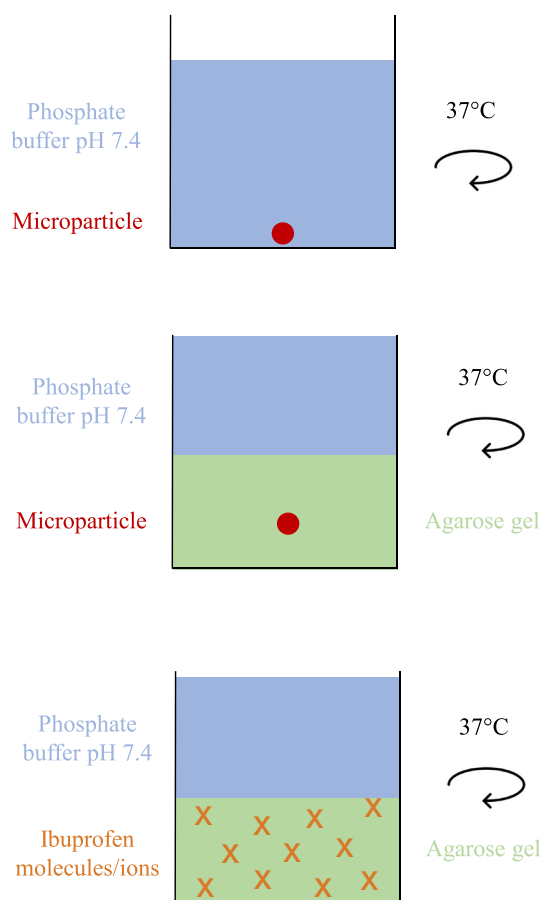


Fig. 1. Schematic presentation of the experimental setups used to monitor drug release from ibuprofen-loaded microparticles: (A) *Bulk fluid setup*: A single microparticle is exposed to 200 μ L phosphate buffer pH 7.4 in a microplate well. (B) *Agarose gel setup*: A single microparticle is embedded within 100 μ L agarose gel, which is exposed to 100 μ L phosphate buffer pH 7.4 in a microplate well. For reasons of comparison, also a reference experiment was conducted: (C) Ibuprofen release was measured from a gel, in which the drug was initially dissolved (the crosses represent individual ibuprofen molecules/ions). In all cases, the microplates were horizontally shaken at 80 rpm and 37 °C.

2. Materials and methods

2.1. Materials

Poly (D,L lactic-co-glycolic acid) (PLGA, 50:50 lactic acid:glycolic acid; Resomer RG 503H; Evonik, Darmstadt, Germany); ibuprofen (BASF, Ludwigshafen, Germany); polyvinyl alcohol (Mowiol 4-88; Sigma-Aldrich, Steinheim, Germany); agarose (genetic analysis grade, gelation temperature = 34.5–37.5 °C; gel strength >1200 g/cm²), potassium dihydrogen orthophosphate and sodium hydroxide (Acros Organics, Geel, Belgium); acetonitrile, ethanol, and dichloromethane (VWR, Fontenay-sous-Bois, France).

2.2. Microparticle preparation

Ibuprofen-loaded microparticles were prepared using an oil-in-water (O/W) solvent extraction/evaporation technique. Five hundred mg PLGA 503H and 500 mg ibuprofen were dissolved in 4 mL dichloromethane. This organic phase was emulsified into 2.5 L of an aqueous poly(vinyl) alcohol (0.25% w/w) solution under stirring (900 rpm, Eurostar power-b; Ika, Staufen, Germany) for 30 min. Upon dichloromethane partitioning into the outer aqueous phase, the PLGA precipitated, and microparticles formed. The latter were hardened by adding

another 2.5 L of the same outer aqueous phase and further stirring at 700 rpm (Eurostar power-b) for 4 h. The microparticles were separated by filtration (Nylon filter, 0.45 μm , 13 mm; GE Healthcare, Kent, UK), washed with demineralized water, and freeze-dried for 3 d (Christ Alpha 2–4 LSC+; Martin Christ, Osterode, Germany) under the following conditions: freezing at $-50\text{ }^{\circ}\text{C}$ for 2.5 h, primary drying at $0\text{ }^{\circ}\text{C}$ and 1 mbar for 34 h, and secondary drying at $20\text{ }^{\circ}\text{C}$ and 0.1 mbar for 34 h. Drug-free microparticles were prepared accordingly, without ibuprofen.

2.3. In vitro drug release

Ibuprofen release into phosphate buffer pH 7.4 (USP 42) was measured from *single* microparticles in 96-well standard microplates (96 well plates; Carl Roth, Karlsruhe, Germany) using the following two experimental setups:

In well-agitated bulk fluid (Fig. 1A): One microparticle was introduced into a well filled with 200 μL phosphate buffer pH 7.4 and sealed with aluminum foil. The microplate was horizontally shaken at 80 rpm and kept at $37\text{ }^{\circ}\text{C}$ (GFL 3033; Gesellschaft fuer Labortechnik, Burgwedel, Germany). At predetermined time points, the entire bulk fluid was carefully replaced by fresh release medium using a Hamilton syringe (Microlite #710, 100 μL ; Hamilton, Bonaduz, Switzerland). The withdrawn samples were analyzed for their drug contents by HPLC-UV analysis, as follows: A Thermo Fisher Scientific Ultimate 3000 Series HPLC apparatus was used, equipped with an LPG 3400 SD/RS pump, an autosampler (WPS-3000 SL) and a UV-Vis detector (VWD-3400RS) (Thermo Fisher Scientific, Waltham, USA). The mobile phase was a 67:33 (v:v) mixture of phosphate buffer pH 6.8 (50 mM KH_2PO_4 and 22.5 mM NaOH) and acetonitrile. Twenty microliter samples were injected into a C18 reversed-phase column (Gemini 5 μm ; 110 \AA ; 150 \times 4.6 mm; Phenomenex, Le Pecq, France). The detection wavelength was 225 nm, and the flow rate was 1 mL/min. Perfect sink conditions were provided throughout the observation periods. Eight microparticles were investigated.

In agarose gel (Fig. 1B): 0.5% w/w agarose gel was prepared by dissolving the polysaccharide in phosphate buffer pH 7.4 (USP 42) under stirring (400 rpm, IKA RCT standard, IKA, Staufen im Breigsau, Germany), gradually increasing the temperature until the liquid boiled. A clear solution was obtained. Fifty microliters of the latter were poured into a well, followed by cooling in a refrigerator for 5 min to allow for gelation. A *single* microparticle was placed in the middle of the gel. Another 50 μL agarose solution was poured into the well (at a temperature far below the boiling point, but sufficiently high to allow pouring the liquid), followed by cooling in a refrigerator for 5 min to allow for gelation. One hundred μL phosphate buffer pH 7.4 were added on top of the gel. The well was sealed with aluminum foil and horizontally shaken at 80 rpm and $37\text{ }^{\circ}\text{C}$ (GFL 3033). At predetermined time points, a Hamilton syringe was used to carefully replace the entire bulk fluid with fresh release medium. The withdrawn samples were analyzed for their drug contents by HPLC-UV analysis, as described above. Perfect sink conditions were provided in the phosphate buffer pH 7.4 (to which the agarose gel was exposed) throughout the observation periods. Eight microparticles were investigated.

It has to be pointed out that the presence of the agarose gel in this setup introduces a bias: The *well-agitated phosphate buffer* is sampled, not the *agarose gel*. Thus, a portion of the drug, which has been released from the microparticles at the time point of sampling, is diffusing through the gel and is not detected as “being released”. To evaluate the importance of this bias, the following two reference experiments were conducted:

(i) 100 μL agarose gels were prepared as described above and exposed to 25 or 100 μL of a solution of ibuprofen in phosphate buffer pH 7.4 (120 $\mu\text{g}/\text{mL}$) in microplate wells for 2 d at $37\text{ }^{\circ}\text{C}$ under horizontal agitation (80 rpm, GFL 3033). This allowed loading the agarose gels with 1.5 or 6 μg ibuprofen, respectively. The drug was dissolved in the gel, as schematically illustrated in Fig. 1C (crosses represent individual ibuprofen molecules/ions). The bulk fluid was replaced by 100 μL fresh

phosphate buffer pH 7.4, and ibuprofen release was measured as described above. Perfect sink conditions were provided in the bulk fluid throughout the observation periods. The experiments were conducted in triplicate, mean values \pm standard deviations are reported.

(ii) As described above, drug release from the PLGA microparticles was measured in agarose gels. After 9 d, the experiments were stopped. The microparticles were separated from the hydrogels. The amount of ibuprofen in the agarose gel was quantified as follows: The gel was manually mixed with 100 μL of a 70:30 (v:v) phosphate buffer pH 7.4: ethanol blend, using a spatula. The slurry was horizontally agitated (80 rpm, GFL 3033) for 2 h at $37\text{ }^{\circ}\text{C}$ to extract the drug. This extraction step was repeated twice with a fresh phosphate buffer pH 7.4:ethanol blend. The bulk fluids were pooled, and their ibuprofen contents were determined by HPLC-UV analysis, as described above. The experiment was conducted eight times. The mean value \pm standard deviation is reported.

2.4. Practical drug loading

The practical ibuprofen loading was determined by dissolving approximately 5 mg microparticles in 5 mL acetonitrile, followed by filtration (PVDF syringe filters, 0.22 μm ; GE Healthcare). The drug content of the solution was determined by HPLC-UV analysis as described above (injecting 10 μL instead of 20 μL samples). The experiments were conducted in triplicate. Mean values \pm standard deviations are reported.

In addition, the drug loading of eight *transparent* and eight *opaque* ibuprofen-loaded microparticles was determined as follows: The microparticles were subjected to the same treatment as for the in vitro drug release measurements described in Section 2.3. At the end of the observation period (when a plateau value was reached), the ibuprofen content of the remaining microparticle remnants (highly swollen gels) was determined as described above and found to be zero in all cases. Thus, the experimentally measured plateau value was considered corresponding to the initial drug content.

2.5. Optical microscopy

Before exposure to the release medium: Pictures of ensembles of microparticles were taken using a Nikon SMZ-U microscope (Tokyo, Japan), equipped with an AxioCam ICc1 camera (Carl Zeiss, Jena, Germany). The Axiovision Zeiss Software was used for data treatment.

After exposure to the release media: Microparticles were treated using the method described for the in vitro drug release studies from *single* microparticles (see Section 2.3.). At predetermined time points, pictures were taken using an Axiovision Zeiss Scope-A1 microscope, equipped with an AxioCam ICc1 camera. The diameters of the microparticles were determined with the Axiovision Zeiss Software.

2.6. Differential scanning calorimetry (DSC)

DSC thermograms of the raw materials (ibuprofen, PLGA) and microparticles were recorded with a DSC1 Star apparatus (Mettler Toledo, Greifensee, Switzerland). Approximately 5 mg samples were heated in perforated aluminum pans from $-70\text{ }^{\circ}\text{C}$ to $120\text{ }^{\circ}\text{C}$, cooled to $-70\text{ }^{\circ}\text{C}$ and reheated to $120\text{ }^{\circ}\text{C}$. All steps were performed at a rate of $10\text{ }^{\circ}\text{C}/\text{min}$. The reported glass temperatures (T_g) were determined from the 1st heating cycles in the case of microparticles (the thermal history being of interest) and from the 2nd heating cycles in the case of the PLGA raw material (the thermal history not being of interest).

2.7. X-ray powder diffraction

X-ray powder diffraction analyses were performed with a Panalytical X'Pert Pro diffractometer equipped with a Cu X-ray tube ($\lambda = 1.54\text{ \AA}$) and Hilgenberg glass capillaries (diameter 0.7 mm) in transmission mode

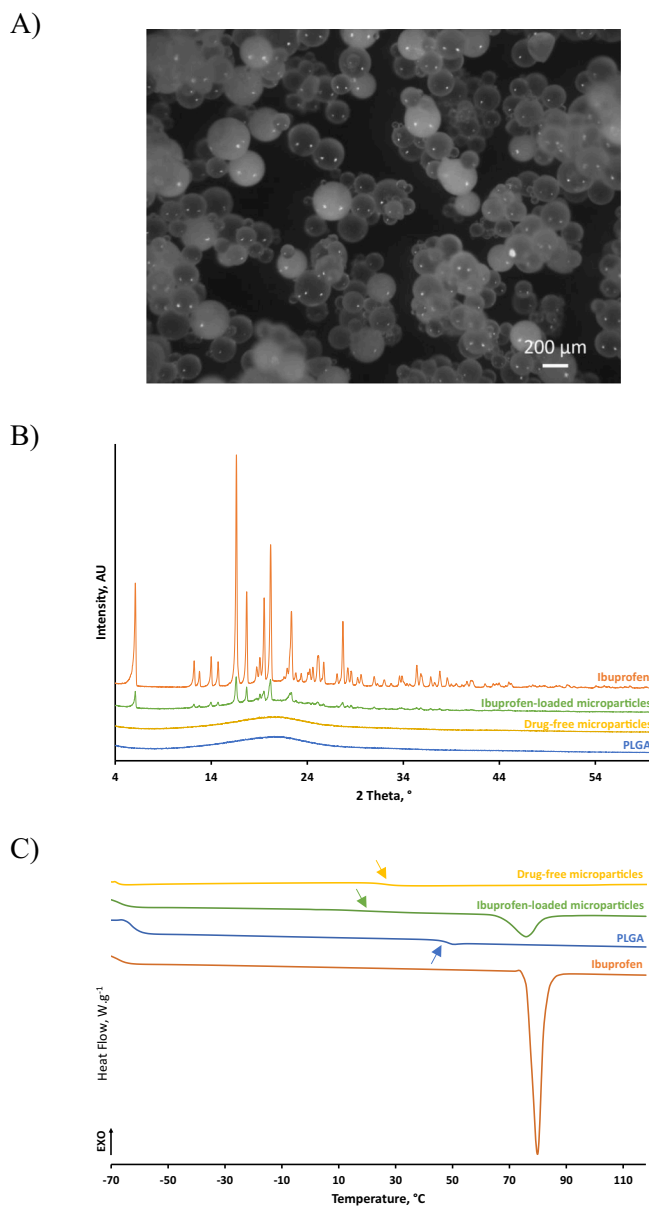


Fig. 2. A) Optical microscopy picture of an ensemble of ibuprofen-loaded microparticles before exposure to release medium. B) X-ray diffraction patterns of the investigated ibuprofen-loaded and drug-free PLGA microparticles before exposure to release medium (*ensembles of transparent and opaque microparticles* were studied). For reasons of comparison, also the X-ray diffraction patterns of the raw materials (PLGA & ibuprofen) are shown. C) DSC thermograms of ibuprofen-loaded PLGA microparticles before exposure to the release medium (1st heating cycle) (*ensembles of transparent and opaque microparticles* were studied). For reasons of comparison, also the DSC thermograms of the raw materials are shown: PLGA (2nd heating cycle) and ibuprofen (1st heating cycle). Flashes highlight glass transition temperatures.

with the X'Celerator detector. The diffractograms were recorded from 4 to 60° (2θ, 0.0167° steps, 50 s step⁻¹).

2.8. Scanning electronic microscopy (SEM)

The microparticles' internal and external morphology before and after exposure to the release medium was studied using a JEOL Field Emission Scanning Electron Microscope (JSM-7800F, Tokyo, Japan). Samples were fixed with a ribbon carbon double-sided adhesive tape and sputter coated with a thin chrome layer. *In case of prior exposure to the*

release medium, the samples were freeze-dried, as described in [Section 2.2](#) before analysis. Cross-sections of the microparticles were obtained upon inclusion into water-based glue (UHU, Bolton Group, Buehl, Germany), drying for 48 h, and slicing with a razor blade or using a cryostat (Leica CM3050 S, Wetzlar, Germany), as indicated.

2.9. X-ray micro computed tomography (X-ray μCT)

X-ray μCT analysis was performed using a SkyScan 1172 micro CT scanner (Bruker, Kontich, Belgium) to characterize the inner structure of the microparticles (before exposure to the release medium) in a non-invasive manner. Samples were placed on a polystyrene support. A camera array with size 4000 × 2672 was used, resulting in a resolution of 2.26 μm. The rotation step was 0.25°.

3. Results and discussion

This study aimed to evaluate the potential impact of the presence of an agarose gel surrounding PLGA-based microparticles on the resulting drug release kinetics. The microparticles were prepared by an oil-in-water (O/W) emulsion solvent extraction/evaporation method. The theoretical ibuprofen loading was 50% (w/w). Importantly, drug release was measured from *single* microparticles to better understand the underlying drug release mechanisms. Resomer RG 503H was selected as PLGA grade (with a 50:50 ratio lactic acid:glycolic acid and acid end groups, Evonik), because a release period of about 2 weeks was targeted.

3.1. Key properties of the microparticles

[Fig. 2A](#) shows an optical microscopy picture of an ensemble of ibuprofen-loaded microparticles. As can be seen, the microparticles were spherical. Interestingly, some of them were *transparent*, while others were *opaque*. This can serve as an indication of the fact that the drug was completely *dissolved* in the polymer in some of the microparticles: the transparent ones. In contrast, in the opaque microparticles, portions of the ibuprofen were likely at least partially present in the form of tiny, amorphous or crystalline, solid particles. The practical drug loading of ensembles of transparent and opaque microparticles was determined to be 47.5 ± 0.4% (5 mg samples were studied). This indicates that the drug loss into the outer aqueous phase during microparticle preparation was only minor (the theoretical drug loading was 50%). Notably, the drug loading was similar for transparent and opaque microparticles. It has previously been reported that the solubility of ibuprofen in this type of PLGA is well below the practical drug loading of the microparticles investigated in this study ([Bassand et al., 2022a](#)). Thus, in the *transparent* microparticles, the polymer matrix can be expected to be oversaturated with the drug, while in *opaque* microparticles the excess of ibuprofen (at least partially) resulted in phase separation and precipitation.

X-ray powder diffraction analysis was applied to better understand the drug's physical state within the microparticles (e.g., amorphous versus crystalline). The green curve in [Fig. 2B](#) shows the diffraction patterns of the drug-loaded microparticles before exposure to the release medium (*ensembles of transparent and opaque microparticles* were studied). For comparison, the raw materials (ibuprofen and PLGA) and drug-free microparticles were also analyzed. As can be seen, the PLGA raw material and drug-free microparticles were X-ray amorphous, while ibuprofen raw material was crystalline. Notably, the ibuprofen-loaded microparticles showed clear diffraction peaks at the same angles as the drug powder raw material. Thus, the *opaque* microparticles in [Fig. 2A](#) likely contain tiny ibuprofen *crystals*, which are distributed throughout the spheres. In addition, a certain portion of the drug can be expected to be *dissolved* in the polymer in these opaque microparticles. Please note that, in addition, it is also possible that parts of the drug are present in the form of *amorphous* particles.

The DSC thermograms illustrated in [Fig. 2C](#) confirm these

Opaque ibuprofen-loaded microparticles (t = 0)

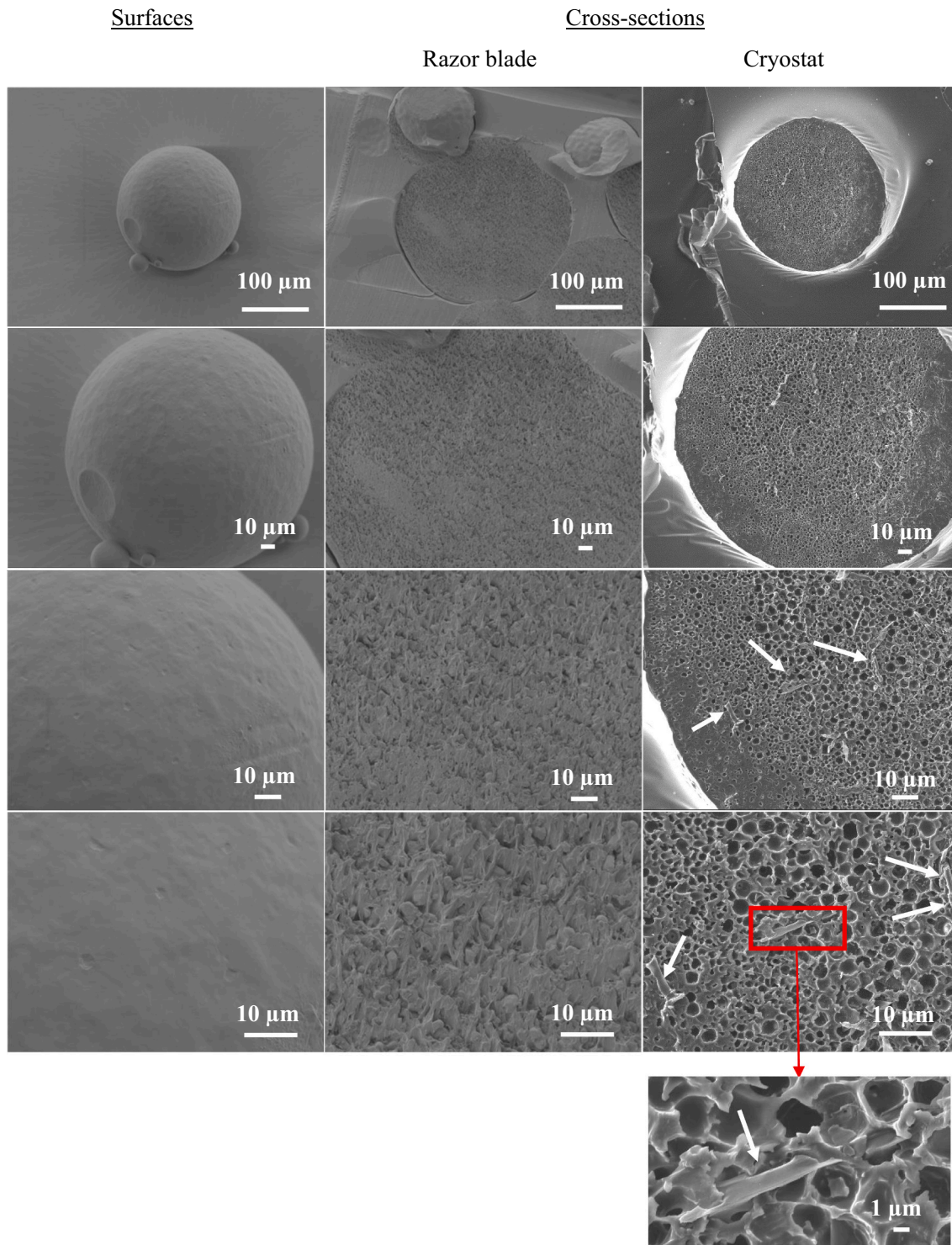


Fig. 3. SEM pictures of *opaque* ibuprofen-loaded microparticles before exposure to release medium: surfaces and cross-sections obtained using a razor blade or cryostat (as indicated). The flashes highlight ibuprofen particles.

hypotheses: The green curve corresponds to drug-loaded microparticles (*ensembles of transparent and opaque microparticles* were studied). The blue and orange curves correspond to the raw materials: PLGA and ibuprofen. In the case of the PLGA raw material, the *second* heating cycle is shown, because the samples' thermal history was not critical (e.g., the polymer was entirely dissolved in dichloromethane during microparticle preparation). In the other cases, the *first* heating cycles are shown. The

orange curve shows a sharp melting peak of crystalline ibuprofen at about 80 °C. The blue curve exhibits a glass transition at about 47 °C, indicating that the polymer was amorphous. Interestingly, its glass transition was decreased to about 20 °C in the ibuprofen-loaded microparticles, probably due to the plasticizing effects of this drug for this polymer (Bassand et al., 2022a) as well as to the plasticizing effects of residual dichloromethane and water (see also the yellow curve in

Transparent ibuprofen-loaded microparticle (t = 0)

Cross-section (Cryostat)

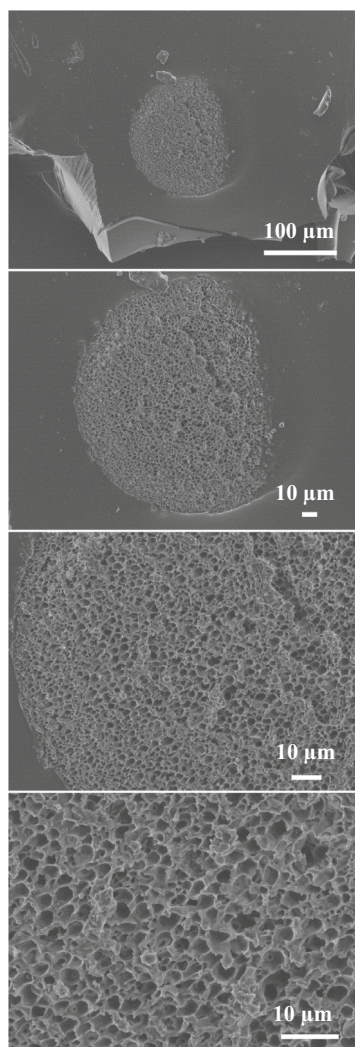


Fig. 4. SEM pictures of a *transparent* ibuprofen-loaded microparticle before exposure to release medium: cross-section obtained using a cryostat, viewed at different degrees of magnification.

Fig. 2C, corresponding to drug-free microparticles). Importantly, a pronounced endothermic peak was observed with the ibuprofen-loaded microparticles, starting at approximately 76 °C. It likely indicates the dissolution of ibuprofen particles in the PLGA and/or melting of the crystalline ibuprofen particles.

SEM pictures of surfaces and cross-sections of *opaque* microparticles further confirm the above-described hypotheses: On the left-hand side of Fig. 3, the surface of a microparticle is shown at different degrees of magnification. Pictures of a cross-section (obtained with a razor blade) through a microparticle are illustrated in the middle panel. The surface of the system was smooth, and no pores were visible. In contrast, the *inner* structure of the microparticle was highly porous. A continuous network of tiny pores goes throughout the entire system. On the right-hand side of Fig. 3, SEM pictures of a cross-section of a microparticle obtained with a *cryostat* are shown. As can be seen, the interconnected pore network is even more evident. At higher magnification, small ibuprofen particles/crystals are visible as well (highlighted by the flashes). Importantly, the latter were homogeneously distributed throughout the entire system and randomly orientated. The observation

that only a few drug crystals were visible in this cross-section might be explained by the fact that a considerable proportion of the ibuprofen was dissolved in this specific microparticle (as discussed above). Also, some drug crystals might have been ejected from the cavities during cutting with the cryostat. Importantly, cross-sections of *transparent* ibuprofen-loaded did not show any evidence for the presence of drug crystals, as illustrated in Fig. 4.

For comparison, the surfaces and cross-sections of *drug-free* microparticles were also studied using SEM. As can be seen in Fig. 5, the placebo microparticles had a smooth, non-porous surface and a dense, non-porous inner structure. The reason for the difference in internal system porosity of “*drug-free versus drug-loaded*” microparticles might be attributable to differences in the solubility of the PLGA in “pure dichloromethane” versus “dichloromethane containing a high concentration of dissolved ibuprofen”. Such differences in polymer solubility might lead to altered PLGA precipitation rates during microparticle formation and, thus, different microparticle morphologies. A more detailed investigation of this phenomenon was beyond the scope of this study. The “structures”, which can be seen in the cross-sections in Fig. 5, are likely artifacts stemming from cutting the microparticles using a razor blade or cryostat. Especially at lower magnification, a preferred orientation of the “lines” perpendicular to the cutting direction can be observed. In contrast, the ibuprofen particles observed in Fig. 3 were randomly orientated; some were needle-shaped.

Since artifacts can be created during the preparation of the samples for SEM analysis (e.g., during cutting), X-ray microcomputed tomography (X-ray μ CT) was also applied to monitor the microparticle morphology. Importantly, this is a non-invasive technique allowing to obtain *virtual* cross-sections of the microparticles. Fig. 6 shows examples of cross-sections of drug-free and ibuprofen-loaded PLGA microparticles (before exposure to the release medium, *ensembles of transparent and opaque* specimen). Clearly, drug-free systems did not show any evidence of the presence of pores. In contrast, ibuprofen-loaded microparticles exhibited a highly porous inner structure, confirming the SEM pictures of “real” cross-sections (right-hand side of Fig. 3). Video 1 shows a series of virtual cross-sections through drug-free loaded microparticles before exposure to the release medium. As can be seen, the inner structure is homogeneous and non-porous. Video 2 shows a series of virtual cross-sections through ibuprofen-loaded microparticles before exposure to the release medium. An *ensemble of transparent and opaque microparticles* is visualized. Pores can be seen throughout the microparticles.

3.2. Drug release kinetics

Fig. 7 shows the experimentally measured drug release kinetics from the investigated ibuprofen-loaded microparticles in the bulk fluid setup (Fig. 1A) and agarose gel setup (Fig. 1B). Mean values \pm standard deviations are plotted ($n = 8$, *transparent and opaque microparticles*). The observed drug release rates were substantially different in the two setups, although the microparticles were from the same batch: Ibuprofen release was much faster into the well-agitated bulk fluid compared to the agarose gel. In addition, the *variability* in drug release was more pronounced upon direct exposure to phosphate buffer compared to inclusion into a hydrogel (mimicking patient tissue).

One of the reasons for the lower release rate observed in the agarose gel setup is the following: Ibuprofen, which is released from the microparticles, is not immediately detected as “being released”: It first has to diffuse through the hydrogel to get into the phosphate buffer, which is sampled and analyzed for its drug content (Fig. 1B). Direct sampling of hydrogel pieces and subsequent drug quantification is possible (Klose et al., 2009), but it is somewhat cumbersome (e.g., it is a destructive sampling method requiring multiple gels for different time points). Thus, at least parts of the released drug remain “undetected” in the agarose gel at the time point of sampling in the setup used in this study. To evaluate the importance of the introduced error, the following two reference experiments were conducted:

Drug-free microparticles (t = 0)

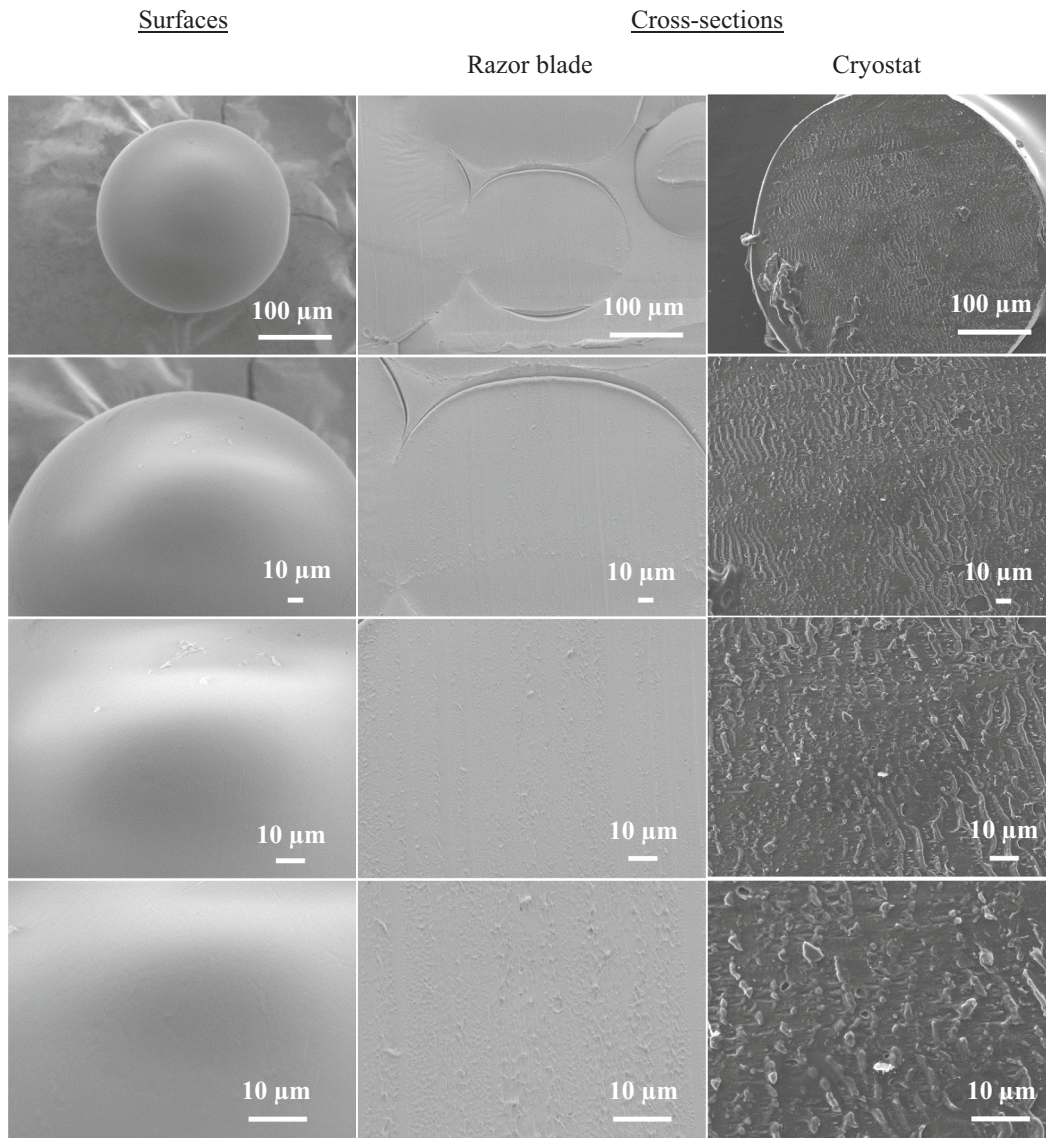


Fig. 5. SEM pictures of drug-free microparticles before exposure to release medium: surfaces and cross-sections obtained using a razor blade or cryostat (as indicated).

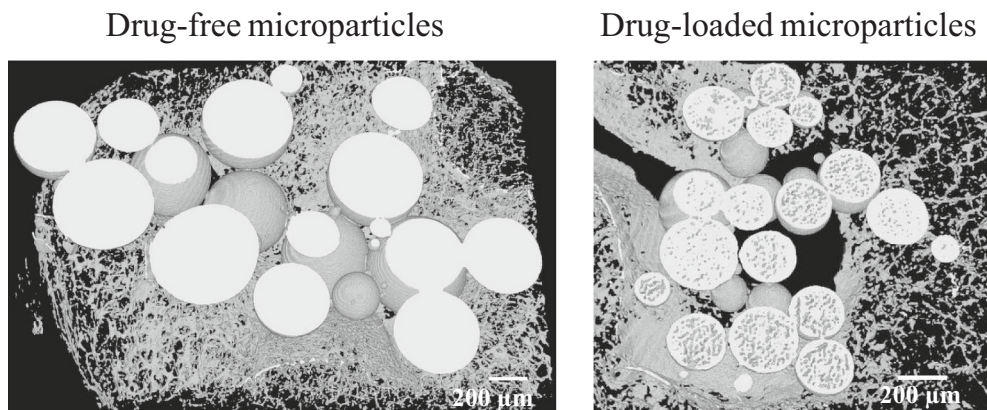


Fig. 6. Virtual cross-sections of drug-free and drug-loaded microparticles (before exposure to release medium) obtained by X-ray μCT (ensembles of transparent and opaque microparticles).

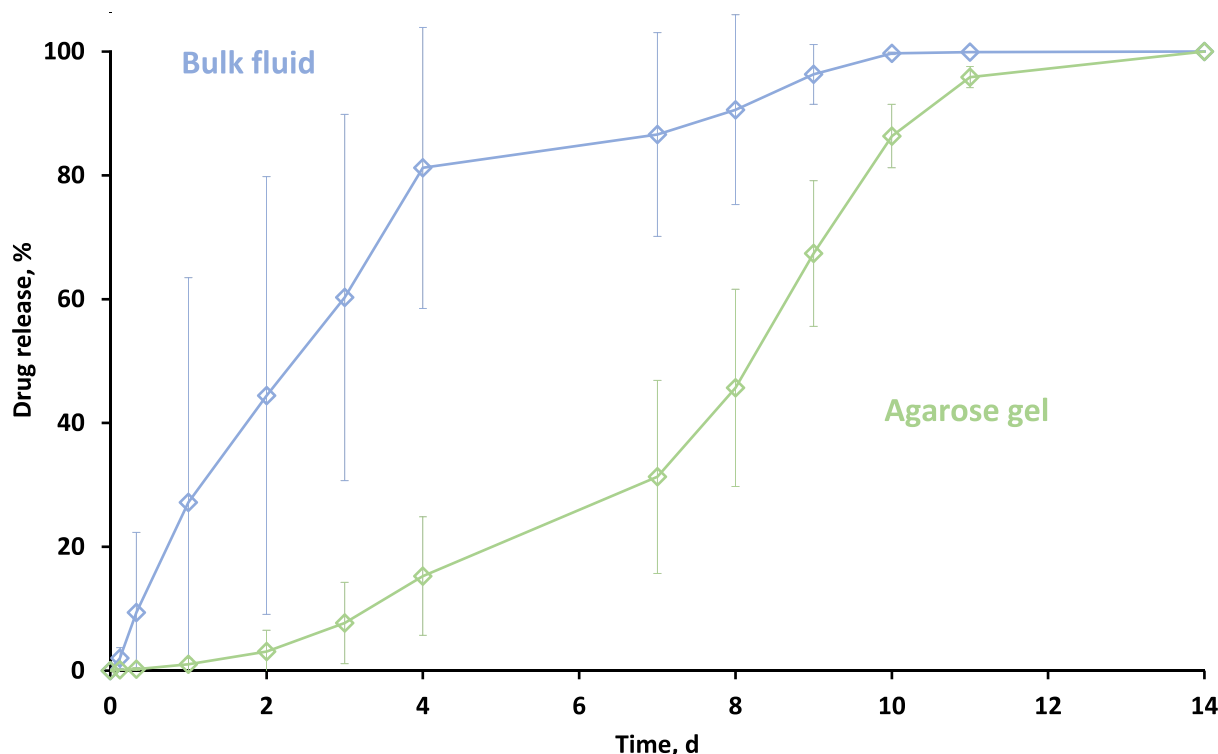


Fig. 7. Ibuprofen release from the investigated PLGA microparticles observed using the agitated bulk fluid setup (Fig. 1A) or the agarose gel setup (Fig. 1B). Mean values \pm standard deviations are illustrated ($n = 8$, transparent and opaque microparticles).

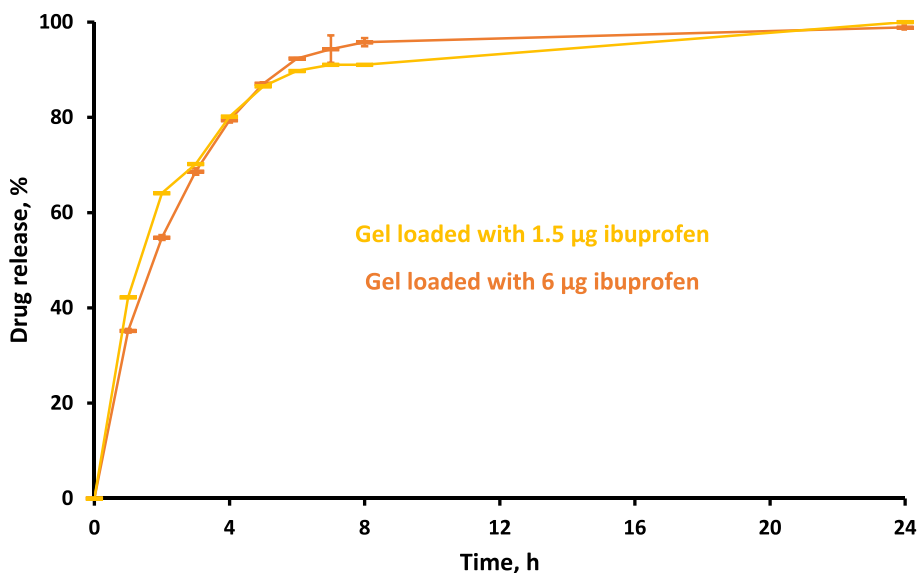


Fig. 8. Ibuprofen release from agarose gels into well-agitated phosphate buffer pH 7.4. The drug was dissolved in the gels. Fig. 1C schematically illustrates the setup. The gels were initially loaded with 1.5 or 6 μg drug (as indicated).

(i) Agarose gels were loaded with 1.5 or 6 μg ibuprofen, being dissolved in the system (initially drug-free gels were exposed to ibuprofen solutions for 2 d). The resulting drug concentrations in the gels represented the ibuprofen concentrations in this phase during the drug release measurements. Ibuprofen release from these gels was measured under the same conditions as for the drug-loaded microparticles (as illustrated in Fig. 1C). Fig. 8 shows the observed release rates. The orange curve corresponds to gels initially loaded with 6 μg drug, and the yellow curve to gels initially loaded with 1.5 μg . As can be seen, the relative release kinetics were similar for both drug loadings, and

ibuprofen release was complete within about 8 h. This indicates that the observed major differences in the release rates of ibuprofen from the investigated microparticles using the bulk fluid versus agarose gel setup can only to a minor/moderate extent be explained by the additional mass transport step through the hydrogel: The difference in drug release is of the order of several days for the microparticles (Fig. 7), compared to about 8 h for complete release from the hydrogel (Fig. 8).

(ii) The “worst case” condition was selected to directly measure the amount of ibuprofen present in the agarose gel at a sampling time point. This was the day with the highest release rate in the agarose setup

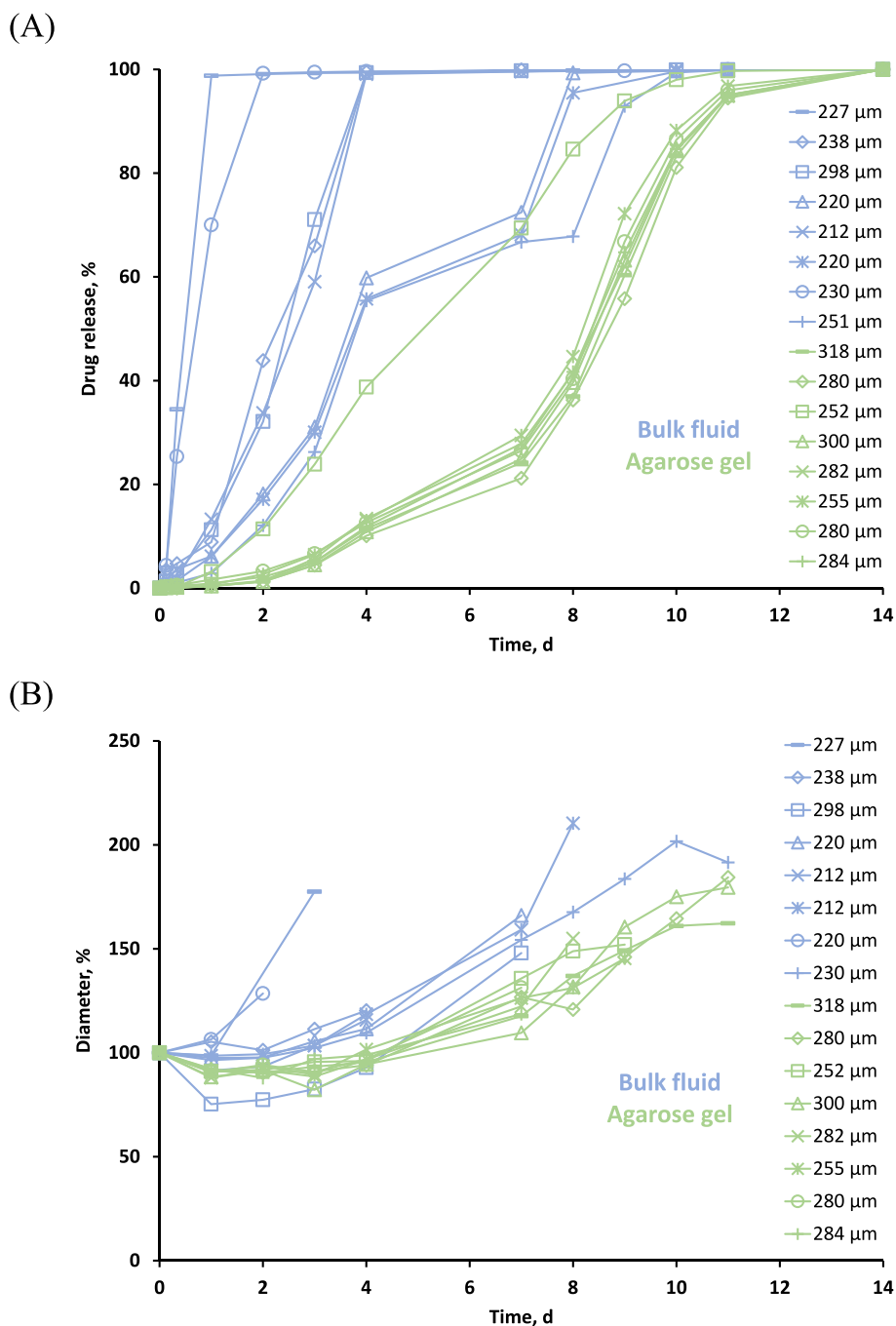


Fig. 9. (A) Ibuprofen release from *single* microparticles into well-agitated phosphate buffer pH 7.4 (blue curves) or agarose gels (green curves). (B) Dynamic changes in the diameters of ibuprofen-loaded microparticles upon exposure to well-agitated phosphate buffer pH 7.4 (blue curves) or agarose gels (green curves). Each curve corresponds to a specific *single* microparticle. The same symbols in (A) and (B) refer to the *same* microparticle. The initial diameters of the microparticles are indicated on the right-hand side. (For interpretation of the references to color in this figure legend, the reader is referred to the web version of this article.)

(steepest slope in Fig. 7): Day 9. Since drug release was fastest on this day, the amount of ibuprofen diffusing through the hydrogel can be expected to be highest. Agarose gel samples were withdrawn that day, and their drug content was determined ($n = 8$). The percentage of the drug “diffusing through the gel” was found to be $17.8 \pm 7.5\%$ ($100\% = \text{total drug loading of the microparticle}$). This confirmed the minor/moderate bias introduced by the experimental setup. Please note that this was the “worst case scenario”, at other time points the relative bias can be expected to be much less important.

The release kinetics of ibuprofen from *single* microparticles are shown in Fig. 9A: The blue curves correspond to the bulk fluid setup, and

the green curves to the agarose setup. Each curve illustrates the release behavior of a specific microparticle (the initial diameter of which is indicated on the right-hand side). As can be seen, the release kinetics of *single* microparticles into *agarose gel* was relatively uniform (most green curves overlap). In contrast, the release patterns of ibuprofen from *single* microparticles into *well-agitated bulk fluid* exhibited a much higher variability (blue curves). To better understand these differences, also the *swelling* kinetics of the microparticles were monitored in the two experimental setups: Fig. 9B shows the dynamic changes in the microparticles' diameters as a function of the exposure time to the bulk fluid (blue curves) or agarose gels (green curves). Note that values above

(A) Agarose gel

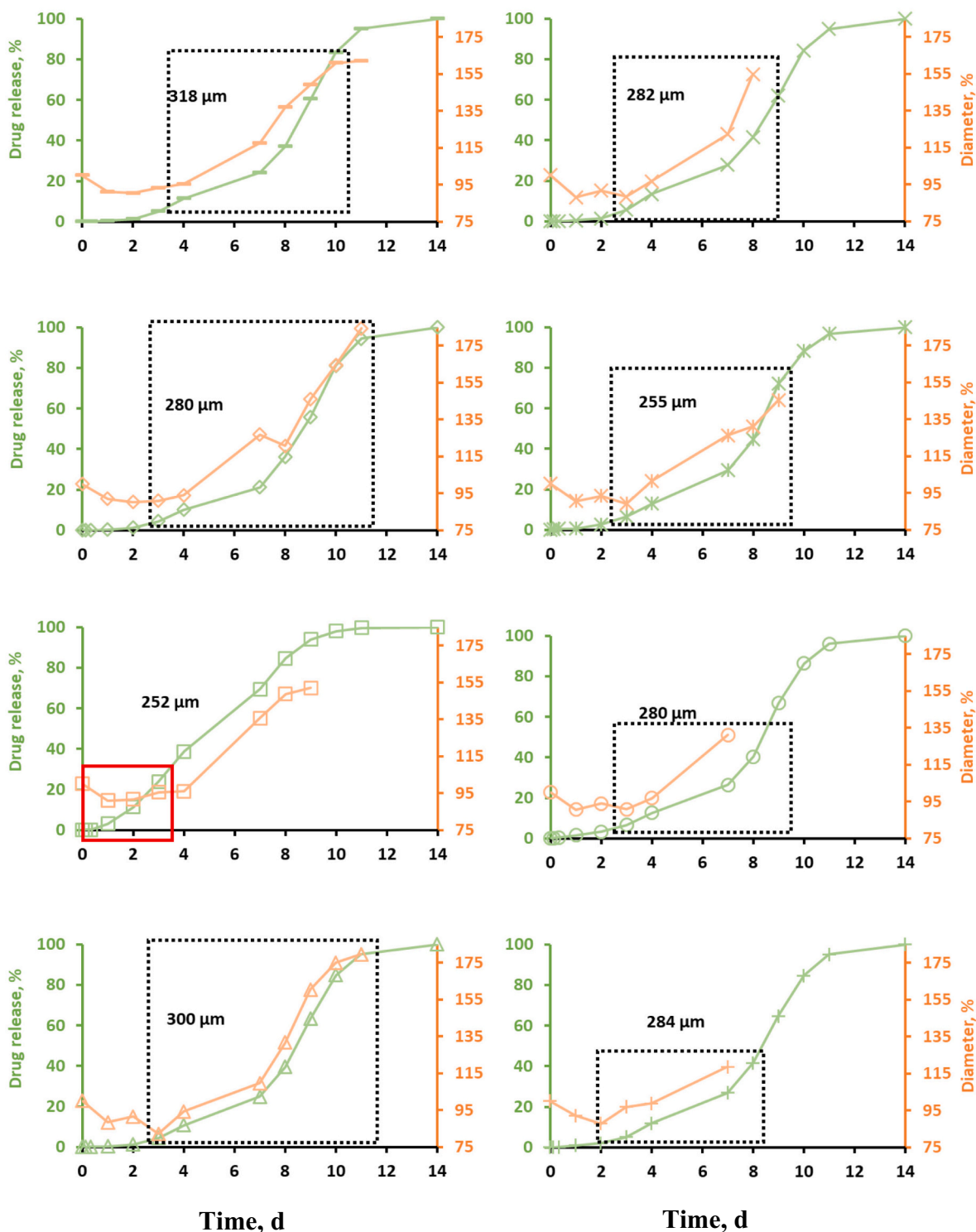


Fig. 10. Ibuprofen release from and swelling kinetics of *single* microparticles observed with the: (A) agarose setup, and (B) bulk fluid setup. Each diagram corresponds to a specific microparticle. The initial microparticle diameter is indicated the diagrams. The green curves illustrate drug release in agarose gels, the blue curves in well-agitated bulk fluid. The orange curves show the swelling kinetics of the microparticles. The dotted black rectangles highlight coinciding onsets of substantial microparticle swelling and drug release. The red rectangles highlight cases, in which drug release set on prior to substantial microparticle swelling. The dotted black ovals highlight cases, in which intermediate plateau values were reached. (For interpretation of the references to color in this figure legend, the reader is referred to the web version of this article.)

(B) Bulk fluid

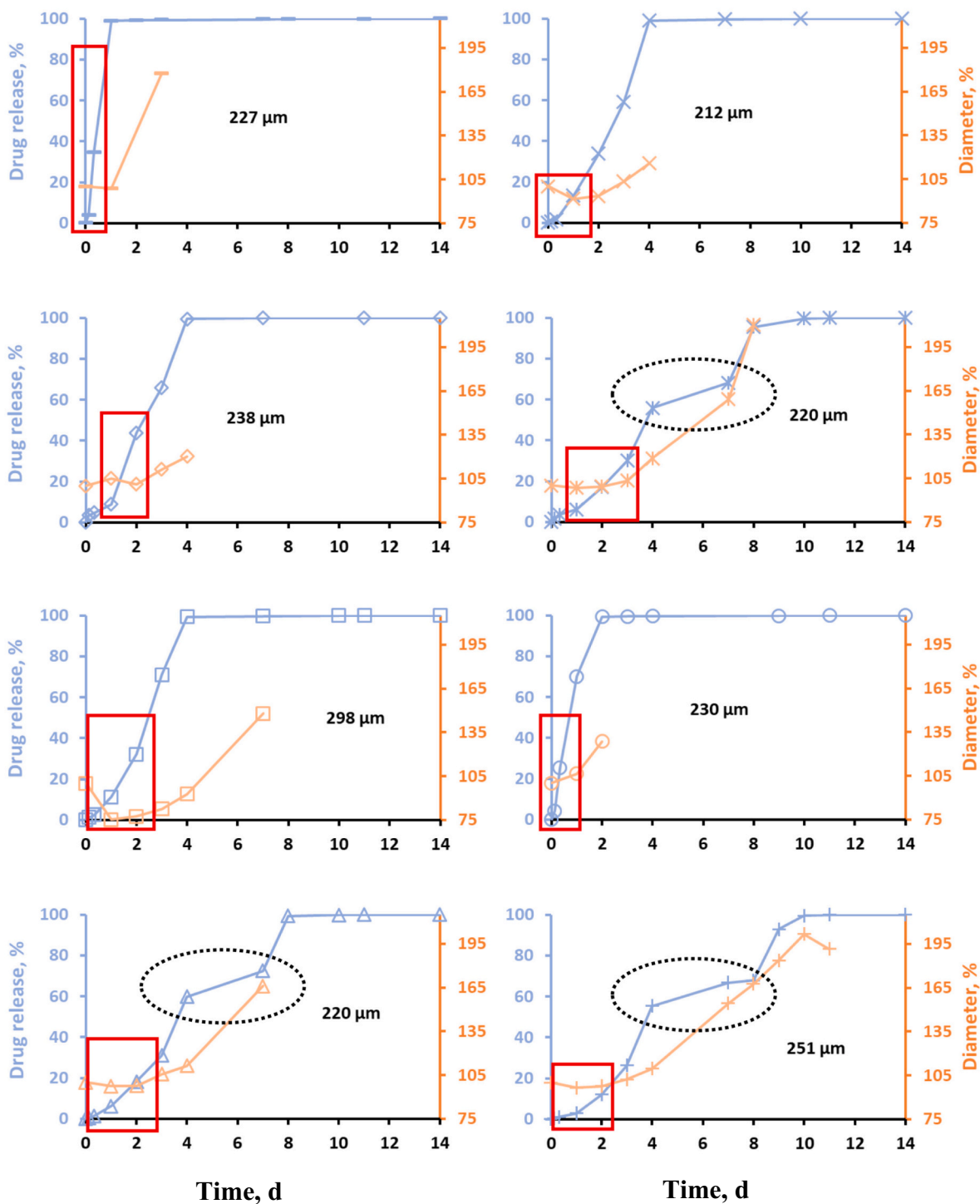


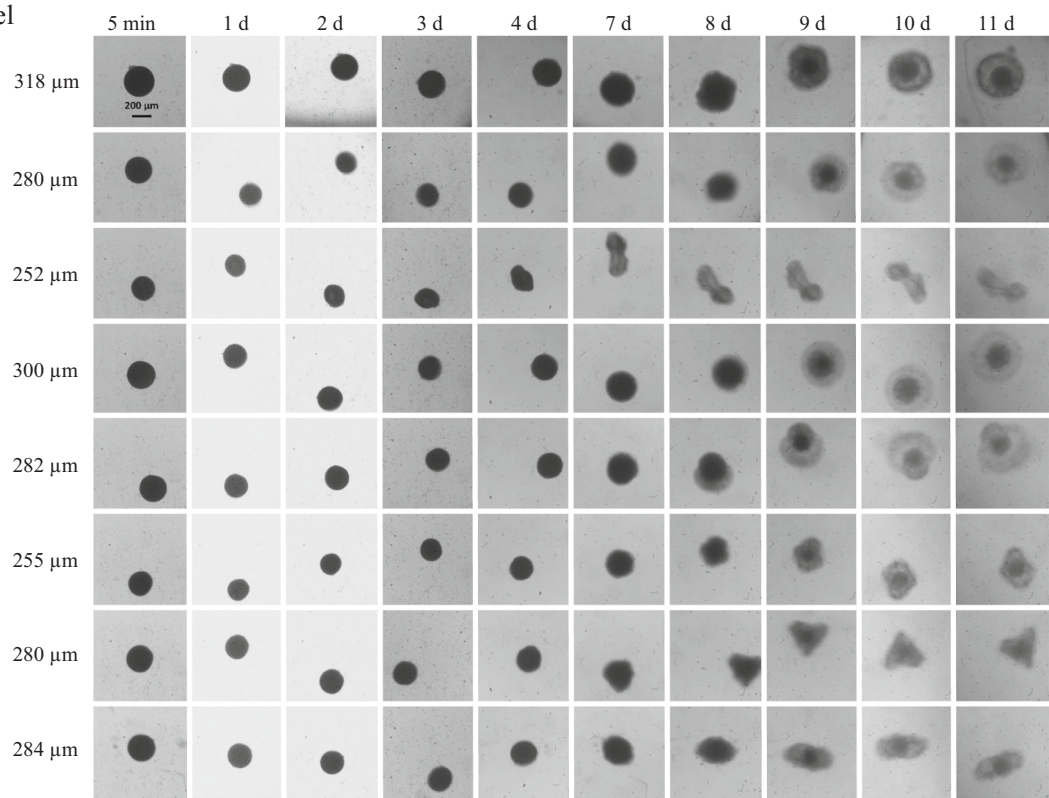
Fig. 10. (continued).

150% should be viewed cautiously, because the microparticles tended not to swell homogeneously in all directions: Instead, a preferential expansion in the plane parallel to the gels' surfaces was observed. This can be explained as follows: First, half of the agarose gel was cast into the well, followed by placing the microparticle in its center, and casting the second half of the agarose gel on top. The cohesion between the bottom and top agarose layers was not as high as the cohesion *within* one of these layers. Consequently, the microparticles encountered less

mechanical resistance when expanding "in between" the two gel layers. The diameters were estimated based on photos taken from the top.

Again, the initial diameters of the single microparticles are indicated on the right-hand side in Fig. 9B. The same symbols are used as in Fig. 9A: Thus, curves with the same color and symbols in Fig. 9A and B illustrate the release and swelling kinetics of the *same single* microparticle. Looking at Fig. 9B, it can be seen that also the *swelling* kinetics of the single microparticles showed limited variability in the agarose setup

A) Agarose gel



(B) Bulk fluid

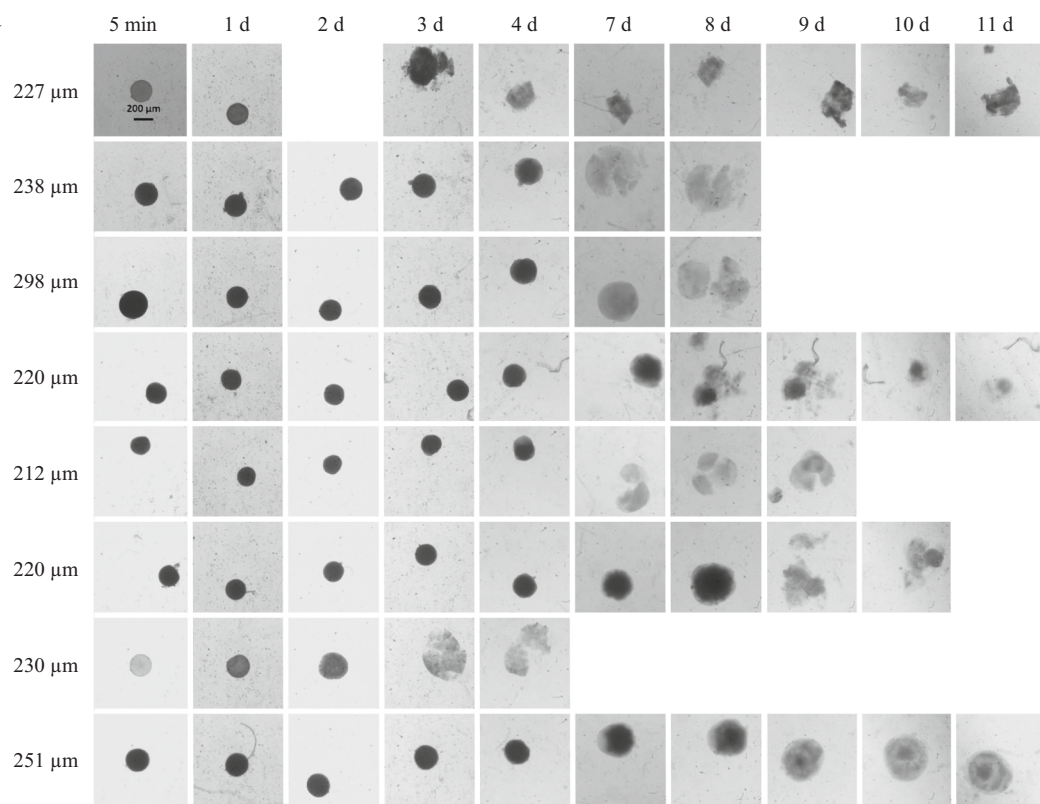


Fig. 11. Optical microscopy pictures of ibuprofen-loaded microparticles upon exposure to: (A) agarose gel, (B) well-agitated phosphate buffer pH 7.4. The exposure times are indicated at the top, the initial microparticle diameters on the left-hand side. Please note that the little dots are dust particles on the lens of the microscope.

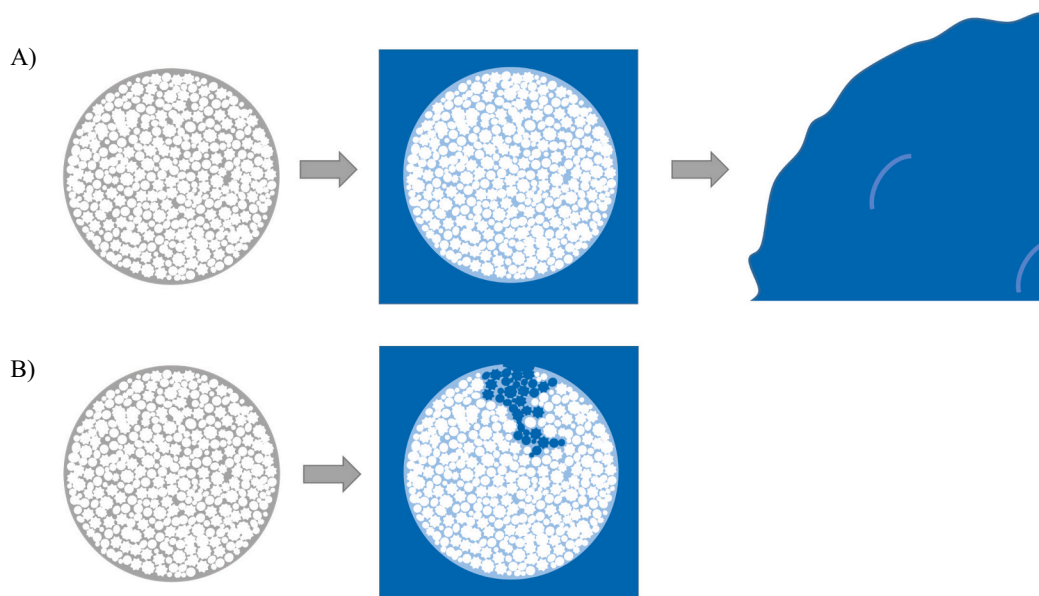


Fig. 12. Schematic illustration of the hypothesized drug release mechanisms: (A) After a certain lag-time (here about 4 d upon exposure to agarose gels), substantial system swelling sets on, leading to fundamentally increasing drug mobility and the onset of ibuprofen release. (B) In certain cases, the continuous pore network gets direct surface access, allowing for the penetration of important amounts of water into the system, followed by drug dissolution and rapid diffusion through water-filled channels.

(green curves), and much higher variability in the bulk fluid setup (blue curves). Thus, a hydrogel surrounding the microparticles substantially delayed both: “drug release & system swelling”, and reduced the variability of the kinetics of these phenomena.

3.3. Drug release mechanisms

Comparing Fig. 9A and B, it can be seen that *overall* there seems to be a rather good correlation between the swelling kinetics of the microparticles and their release behavior, especially for the agarose gel set-up. To allow for a direct comparison between the drug release and swelling kinetics of *single* microparticles, the results were plotted differently in Fig. 10: Each diagram illustrates the behavior of one specific microparticle. The green and blue curves correspond to the left y-axes and show the observed drug release rates. The orange curves correspond to the right y-axes and illustrate the swelling kinetics (again, values above about 150% in agarose gels should be viewed with caution). The green color refers to the agarose setup (Fig. 1B), while the blue color refers to the bulk fluid setup (Fig. 1A).

Looking at the orange curves in Fig. 10A, it can be seen that all microparticles started to swell substantially after about 4 d exposure to agarose gels. This period coincided with the onset of substantial drug release from most of the microparticles (green curves in Fig. 10A). It has previously been hypothesized that the considerable swelling of PLGA-based implants and microparticles is the root cause for the onset of the final, rapid drug release phase from these systems, leading to complete drug exhaust (Bode et al., 2019; Gasmí et al., 2015a, 2015b). Upon exposure to aqueous media, water rather rapidly penetrates the devices, wetting the entire implant or microparticle (e.g., during the first day). However, the polymer is relatively hydrophobic at this stage, and only limited amounts of water are present in the systems (e.g., a few percent). These (even limited) amounts of water lead to hydrolytic polyester bond cleavage throughout the drug delivery systems (“bulk degradation”). Importantly, each hydrolytic cleavage of an ester bond generates two new *hydrophilic* end groups: an -OH and a -COOH group. Thus, with time the polymeric matrices become more and more water-loving. In addition, the polymer molecular weight decreases and, thus, the degree of macromolecular chain entanglement decreases. Hence, the mechanical

resistance to substantial system swelling decreases. Furthermore, water-soluble degradation products (short chain acids) are generated, creating a steadily increasing osmotic pressure in the systems. At a specific timepoint (once a critical polymer molecular weight is reached), substantial system swelling sets on, and the implants and microparticles are transformed into highly swollen PLGA gels. This was confirmed by optical microscopy in the present study: Fig. 11 shows images of microparticles exposed to: (A) agarose gels or (B) well-agitated phosphate buffer at different time points (indicated at the top). After a specific lag time, the microparticles are transformed into highly swollen gels. This fundamentally impacts the drug: Its mobility drastically increases, resulting in accelerated drug release rates. This release mechanism (schematically illustrated in Fig. 12A) also seems dominant for the investigated PLGA microparticles in this study upon exposure to *agarose gels* (dotted black rectangles in Fig. 10A). However, there was one exception, highlighted by the red rectangle in Fig. 10A: In this case, drug release started before the onset of substantial microparticle swelling (the corresponding optical microscopy pictures are shown in the 3rd row in Fig. 11A). This might be explained by the fact that direct surface access was provided to the continuous inner pore network at this time point, allowing considerable amounts of water to penetrate the system. Ibuprofen particles can be expected to rapidly dissolve in this liquid and subsequently diffuse through the water-filled channels out of the microparticles. This release mechanism is schematically illustrated in Fig. 12B.

Fig. 10B shows the behaviors of single microparticles upon exposure to *well-agitated bulk fluid*: Interestingly, in all cases, drug release started before the onset of substantial system swelling, as highlighted by the red rectangles. Thus, upon exposure to well-agitated phosphate buffer pH 7.4, the probability that direct surface access is provided to the continuous inner pore network, is higher than in an agarose gel. This might be explained by the higher mechanical stress encountered by the thin outer PLGA layer, being exposed to an environment with considerable convective liquid flow. In contrast, such mechanical stress is virtually zero for a microparticle embedded in the middle of an agarose gel. SEM pictures of surfaces of drug-loaded microparticles, which had been exposed to agarose gel or well-agitated phosphate buffer for 1 d, seem to confirm this hypothesis: As can be seen in Fig. 13, numerous tiny

Ibuprofen-loaded microparticles (t = 1d)

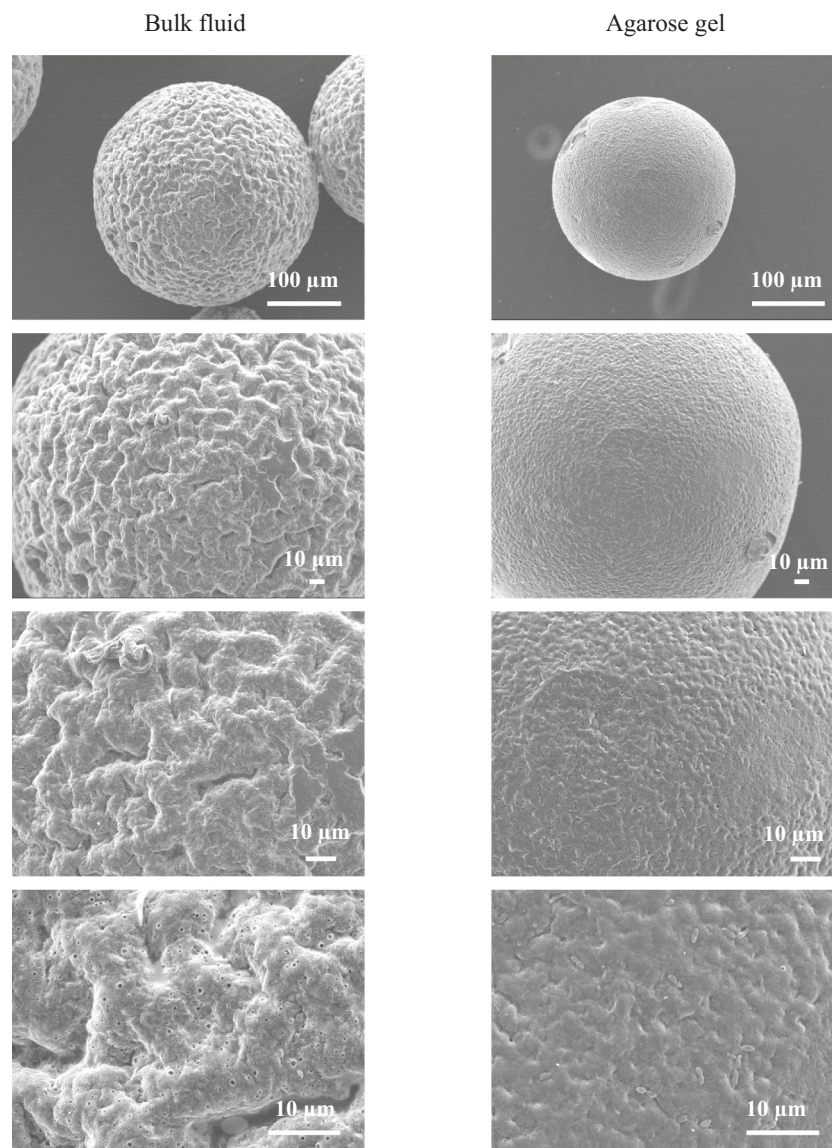


Fig. 13. SEM pictures of surfaces of ibuprofen-loaded microparticles after 1 d exposure to well-agitated bulk fluid or agarose gel.

pores are visible at the surface of a microparticle, which had been exposed to well-agitated bulk fluid. In contrast, less evidence for surface pores is apparent upon exposure to an agarose gel. Please note that great care has to be taken with these SEM pictures, because the samples were freeze-dried before analysis. This results in artifacts such as, e.g., collapsed swollen polymer surface layers.

It must be pointed out that in some instances, direct surface access does not lead to rapid, *complete* drug release. Instead, some plateau values are reached (highlighted by the dotted black ovals in Fig. 10B). This likely indicates that the pore networks in these microparticles are not fully interconnected. Parts of the microstructure within the particle matrix seem to be less well connected. Without direct surface access, drug located in these regions “has to wait” for substantial system swelling to become sufficiently mobile to be released. The fact that the creation of direct surface access to the pore network occurs “occasionally” can explain the observed high variability in the drug release patterns of single microparticles in this experimental setup (discussed above, Fig. 9).

Furthermore, comparing the microparticle swelling kinetics in agarose gels and well-agitated bulk fluid (green and blue curves in Fig. 9), it becomes evident that the presence of the hydrogel delays the onset of substantial microparticle swelling. The mechanical hindrance of substantial microparticle expansion by the gel can explain this.

Please note that the type of experimental set-up might also affect the micro-pH in the vicinity of the microparticles. A surrounding agarose gel can be expected to slow down the neutralization of hydronium ions generated upon dissolution of the acid ibuprofen and upon ester hydrolysis (polymer degradation). Consequently, the solubility of ibuprofen (being pH dependent) might locally drop, leading to potentially *slower* drug release. In addition, PLGA hydrolysis might be accelerated, resulting in potentially *faster* drug release. A detailed investigation of these aspects was beyond the scope of this study.

Fig. 9B illustrates that two specific microparticles showed an exceptionally early onset of substantial system swelling in the bulk fluid setup: The blue curves marked by open circles and horizontal dashes, respectively. This might be explained as follows: As can be seen, in

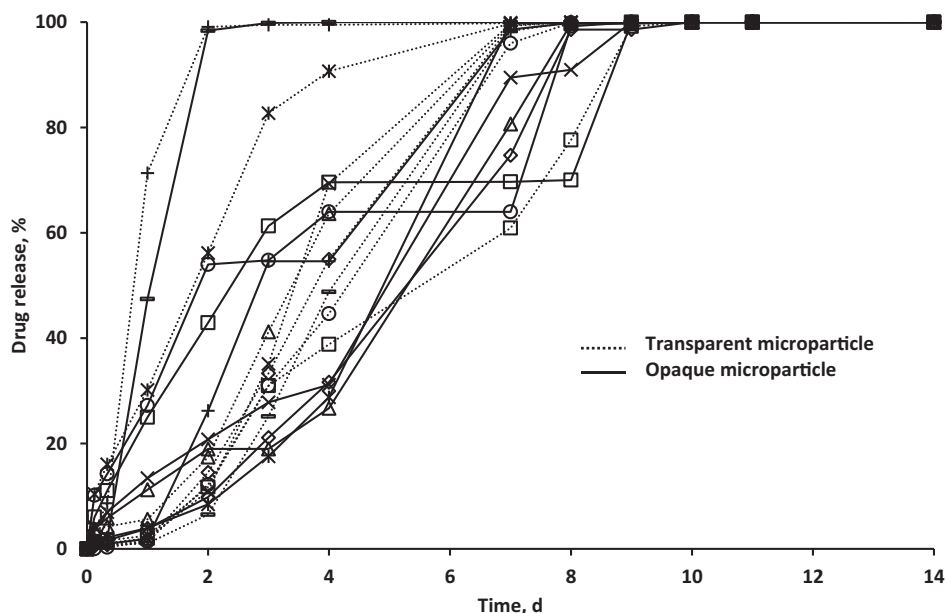


Fig. 14. Ibuprofen release from initially transparent and opaque microparticles (see also Fig. 2A) upon exposure to agarose gels or well-agitated phosphate buffer pH 7.4.

Fig. 9A, for these two microparticles, drug release commences almost instantaneously upon exposure to the well-agitated phosphate buffer. Thus, in these cases, completely interconnected pore networks got probably very rapidly direct surface access (which can at least partially be explained by the higher drug loadings of these microparticles: 58 and 65%). Hence, considerable amounts of water were able to penetrate these systems, and the drug was rapidly released. Due to the high drug loadings and release rates in these cases, the PLGA in these microparticles was exposed to much higher water quantities in the first 2 d compared to the other microparticles. Consequently, hydrolytic ester bond cleavage was faster, and the critical polymer molecular weight at which substantial system swelling commenced, was reached earlier (Fig. 9B). So, for these two microparticles, PLGA swelling was not the root cause for the onset of drug release. Instead, early and complete drug release accelerated system swelling.

As discussed above, some microparticles were transparent, and others were opaque before exposure to the release media (Fig. 2A). Importantly, this difference did not affect the resulting drug release kinetics, as illustrated in Fig. 14: The solid curves correspond to initially opaque microparticles, and the dotted curves to initially transparent ones. This can at least partially be explained by the fact that the transparent microparticles rapidly became opaque upon exposure to the release media (agarose gels or well-agitated bulk fluid), as illustrated, for instance, in the second row from the bottom in Fig. 11B. Thus, upon penetration of (even limited amounts of) water into the microparticles, ibuprofen rapidly precipitated from oversaturated systems, probably because the water increased the mobility of the drug molecules.

4. Conclusions

A surrounding agarose gel (mimicking living tissue) can sterically hinder the swelling of PLGA microparticles and, thus, slow down drug release. In addition, convective liquid flow in well-agitated bulk fluids can likely damage thin PLGA layers at the microparticles' surface and provide more rapid direct surface access to inner pore networks. For these (and other) reasons, great caution should be paid when predicting drug release from PLGA microparticles in vivo, based on in vitro data.

Supplementary data to this article can be found online at <https://doi.org/10.1016/j.ijpx.2023.100220>.

CRediT authorship contribution statement

L.A. Lefol: Investigation, Methodology, Validation, Visualization, Writing – original draft. **P. Bawuah:** Investigation, Methodology, Validation, Visualization, Writing – review & editing. **J.A. Zeitler:** Conceptualization, Funding acquisition, Investigation, Methodology, Project administration, Resources, Supervision, Validation, Visualization, Writing – review & editing. **J. Verin:** Investigation, Methodology, Visualization. **F. Danede:** Investigation, Methodology, Validation, Visualization. **J.F. Willart:** Conceptualization, Investigation, Methodology, Validation, Visualization, Writing – review & editing. **F. Siepmann:** Conceptualization, Funding acquisition, Methodology, Project administration, Resources, Supervision, Validation, Visualization, Writing – review & editing. **J. Siepmann:** Conceptualization, Funding acquisition, Methodology, Project administration, Resources, Supervision, Validation, Visualization, Writing – review & editing.

Declaration of Competing Interest

The authors declare the following financial interests/personal relationships which may be considered as potential competing interests.

Juergen Siepmann reports financial support was provided by Interreg 2 Seas programme. Juergen Siepmann reports financial support was provided by European Regional Development Fund. Axel Zeitler reports financial support was provided by Interreg 2 Seas programme. Axel Zeitler reports financial support was provided by European Regional Development Fund. The Editor-in-Chief of the journal (Juergen Siepmann) is one of the co-authors of this article. Also, one of the guest editors of this special issue (Axel Zeitler) is one of the co-authors of this article. The manuscript has been subject to all of the journal's usual procedures, including peer review, which has been handled independently of the Editor-in-Chief and of the guest editor Axel Zeitler.

Data availability

Data will be made available on request.

Acknowledgments

This project has received funding from the Interreg 2 Seas

programme 2014-2020 co-funded by the European Regional Development Fund under subsidy contract "Site Drug 2S07-033".

References

- Amoyav, B., Benny, O., 2019. Microfluidic based fabrication and characterization of highly porous polymeric microspheres. *Polymers* 11 (3). <https://doi.org/10.3390/polym11030419>.
- Anderson, J.M., Shive, M.S., 2012. Biodegradation and biocompatibility of PLA and PLGA microspheres. *Adv. Drug Deliv. Rev.* 64 (SUPPL), 72–82. <https://doi.org/10.1016/j.addr.2012.09.004>.
- Arpagaus, C., 2019. PLA/PLGA nanoparticles prepared by nano spray drying. *J. Pharm. Investig.* 49 (4), 405–426. <https://doi.org/10.1007/s40005-019-00441-3>.
- Bassand, C., Benabed, L., Verin, J., Danede, F., Lefol, L.A., Willart, J.F., Siepmann, F., Siepmann, J., 2022a. Hot melt extruded PLGA implants loaded with ibuprofen: how heat exposure alters the physical drug state. *J. Drug Deliv. Sci. Technol.* 1–36.
- Bassand, C., Verin, J., Lamatsch, M., Siepmann, F., Siepmann, J., 2022b. How agarose gels surrounding PLGA implants limit swelling and slow down drug release. *J. Control. Release* 343 (January), 255–266. <https://doi.org/10.1016/j.jconrel.2022.01.028>.
- Benhabbour, S.R., Kovarova, M., Jones, C., Copeland, D.J., Shrivastava, R., Swanson, M. D., Sykes, C., Ho, P.T., Cottrell, M.L., Sridharan, A., Fix, S.M., Thayer, O., Long, J.M., Hazuda, D.J., Dayton, P.A., Mumper, R.J., Kashuba, A.D.M., Garcia, J.V., 2019. Ultra-long-acting tunable biodegradable and removable controlled release implants for drug delivery. *Nat. Commun.* 2019 <https://doi.org/10.1038/s41467-019-12141-5>.
- Berkland, C., King, M., Cox, A., Kim, K., Pack, D.W., 2002. Precise control of PLG microsphere size provides enhanced control of drug release rate. *J. Control. Release* 82 (1), 137–147. [https://doi.org/10.1016/S0168-3659\(02\)00136-0](https://doi.org/10.1016/S0168-3659(02)00136-0).
- Blasi, P., D'Souza, S.S., Selmin, F., DeLuca, P.P., 2005. Plasticizing effect of water on poly (lactide-co-glycolide). *J. Control. Release* 108 (1), 1–9. <https://doi.org/10.1016/j.jconrel.2005.07.009>.
- Blasi, P., Schoubben, A., Giovagnoli, S., Perioli, L., Ricci, M., Rossi, C., 2007. Ketoprofen poly(lactide-co-glycolide) physical interaction. *AAPS PharmSciTech* 8 (2), 1–8. <https://doi.org/10.1208/pt080207>.
- Bode, C., Kranz, H., Fizev, A., Siepmann, F., Siepmann, J., 2019. Often neglected: PLGA/PLA swelling orchestrates drug release: HME implants. *J. Control. Release* 306 (May), 97–107. <https://doi.org/10.1016/j.jconrel.2019.05.039>.
- Brunner, A., Mäder, K., Göpferich, A., 1999. pH and osmotic pressure inside biodegradable microspheres during erosion. In: *Pharmaceutical Research*, 16, issue 6, pp. 847–853. <https://doi.org/10.1023/A:1018822002353>.
- Donnell, P.B.O., McGinity, J.W., 1997. Preparation of microspheres by the solvent evaporation technique. *Adv. Drug Deliv. Sci.* 28, 25–42.
- Dorta, M.J., Santoveña, A., Llabrés, M., Fariña, J.B., 2002. Potential applications of PLGA film-implants in modulating in vitro drug release. *Int. J. Pharm.* 248 (1–2), 149–156. [https://doi.org/10.1016/S0378-5173\(02\)00431-3](https://doi.org/10.1016/S0378-5173(02)00431-3).
- Feng, L., Ward, A., Li, J., Tolia, S.K., Hao, J.G., Choo, D.I., 2014. Assessment of PLGA-PEG-PLGA Copolymer Hydrogel for Sustained Drug delivery in the ear. *Curr. Drug Deliv.* 11 (2), 279–286.
- Ford, N., Versypt, A., Pack, W., Braatz, R.D., 2013. Mathematical Modeling of Drug delivery from Autocatalytically Degradable PLGA Microspheres—a Review. *J. Control. Release* 23 (1), 1–7. <https://doi.org/10.1016/j.jconrel.2012.10.015>.
- Fredenberg, S., Wahlgren, M., Reslow, M., Axelsson, A., 2011. The mechanisms of drug release in poly(lactic-co-glycolic acid)-based drug delivery systems - a review. *Int. J. Pharm.* 415 (1–2), 34–52. <https://doi.org/10.1016/j.ijpharm.2011.05.049>.
- Fu, K., Pack, D.W., Klibanov, A.M., Langer, R., 2000. Visual evidence of Acidic Environment within Degrading. *Pharm. Res.* 17 (1), 100–106.
- Gasmi, H., Danede, F., Siepmann, J., Siepmann, F., 2015a. Does PLGA microparticle swelling control drug release? New insight based on single particle swelling studies. *J. Control. Release* 213, 120–127. <https://doi.org/10.1016/j.jconrel.2015.06.039>.
- Gasmi, H., Willart, J.F., Danede, F., Hamoudi, M.C., Siepmann, J., Siepmann, F., 2015b. Importance of PLGA microparticle swelling for the control of prilocaine release. *J. Drug Deliv. Sci. Technol.* 30, 123–132. <https://doi.org/10.1016/j.jddst.2015.10.009>.
- Gasmi, H., Siepmann, F., Hamoudi, M.C., Danede, F., Verin, J., Willart, J.F., Siepmann, J., 2016. Towards a better understanding of the different release phases from PLGA microparticles: Dexamethasone-loaded systems. *Int. J. Pharm.* 514 (1), 189–199. <https://doi.org/10.1016/j.ijpharm.2016.08.032>.
- Ghalanbor, Z., Körber, M., Bodmeier, R., 2012. Protein release from poly (lactide-co-glycolide) implants prepared by hot-melt extrusion : Thioester formation as a reason for incomplete release. *Int. J. Pharm.* 438 (1–2), 302–306. <https://doi.org/10.1016/j.ijpharm.2012.09.015>.
- Guo, T., Lim, C., Noshin, M., Ringel, P.J., Fisher, J.P., 2019. 3D Printing Bioactive PLGA Scaffolds Using DMSO as a Removable Solvent. <https://doi.org/10.1016/j.bprint.2018.e00038.3D>.
- Hirenkumar, M., Steven, S., 2012. Poly Lactic-co-Glycolic Acid (PLGA) as Biodegradable Controlled Drug delivery carrier. *Polymers* 3 (3), 1–19. <https://doi.org/10.3390/polym3031377.Poly>.
- Kang, J., Schwendeman, S.P., 2007. Pore closing and opening in biodegradable polymers and their effect on the controlled release of proteins. *Mol. Pharm.* 4 (1), 104–118. <https://doi.org/10.1021/mp060041n>.
- Kim, H.K., Chung, H.J., Park, T.G., 2006. Biodegradable polymeric microspheres with "open/closed" pores for sustained release of human growth hormone. *J. Control. Release* 112 (2), 167–174. <https://doi.org/10.1016/j.jconrel.2006.02.004>.
- Klose, D., Siepmann, F., Elkharraz, K., Krenzlin, S., Siepmann, J., 2006. How porosity and size affect the drug release mechanisms from PLGA-based microparticles. *Int. J. Pharm.* 314 (2), 198–206. <https://doi.org/10.1016/j.ijpharm.2005.07.031>.
- Klose, D., Azaroual, N., Siepmann, F., Vermeersch, G., Siepmann, J., 2009. Towards more realistic in vitro release measurement techniques for biodegradable microparticles. *Pharm. Res.* 26 (3), 691–699. <https://doi.org/10.1007/s11095-008-9747-4>.
- Kozák, J., Rabišková, M., Lamprecht, A., 2021. In-vitro drug release testing of parenteral formulations via an agarose gel envelope to closer mimic tissue firmness. *Int. J. Pharm.* 594 (August 2020) <https://doi.org/10.1016/j.ijpharm.2020.120142>.
- Lagrega, E., Onesto, V., Di, C., La, S., Paolo, M., Netti, A., 2020. Recent advances in the formulation of PLGA microparticles for controlled drug delivery. *Progress Biomater.* 9 (4), 153–174. <https://doi.org/10.1007/s40204-020-00139-y>.
- Li, Z., Mu, H., Weng Larsen, S., Jensen, H., Østergaard, J., 2021. An in vitro gel-based system for characterizing and predicting the long-term performance of PLGA in situ forming implants. *Int. J. Pharm.* 609 (October) <https://doi.org/10.1016/j.ijpharm.2021.121183>.
- Liu, Y., Ghassemi, A.H., Hennink, W.E., Schwendeman, Steven P., 2008. The microclimate pH in poly(D,L-lactide-co-hydroxymethyl glycolide) microspheres during biodegradation. *Bone* 23 (1), 1–7. <https://doi.org/10.1016/j.biomaterials.2012.06.013.The>.
- Mirzaeei, S., Mansurian, M., Asare-Addo, K., Nokhodchi, A., 2021. Metronidazole-and amoxicillin-loaded plga and pcl nanofibers as potential drug delivery systems for the treatment of periodontitis: in vitro and in vivo evaluations. *Biomedicines* 9 (8). <https://doi.org/10.3390/biomedicines9089075>.
- Park, K., Otto, A., Sharifi, F., Garner, J., Skidmore, S., Park, H., Jhon, Y.K., Qin, B., Wang, Y., 2021. Formulation composition, manufacturing process, and characterization of poly(lactide-co-glycolide) microparticles. *J. Control. Release* 329, 1150–1161. <https://doi.org/10.1016/j.jconrel.2020.10.044>.
- Pean, J.M., Venier-Julienne, M.C., Boury, F., Menei, P., Denizot, B., Benoit, J.P., 1998. NGF release from poly(D,L-lactide-co-glycolide) microspheres. Effect of some formulation parameters on encapsulated NGF stability. *J. Control. Release* 56 (1–3), 175–187. [https://doi.org/10.1016/S0168-3659\(98\)00086-8](https://doi.org/10.1016/S0168-3659(98)00086-8).
- Qi, P., Bu, R., Zhang, H., Yin, J., Chen, J., Zhang, A., Gou, J., Yin, T., Zhang, Y., He, H., Wang, P., Tang, X., Wang, Y., 2019. Goserelin Acetate Loaded Poloxamer Hydrogel in PLGA Microspheres : Core – Shell Di-Depot Intramuscular Sustained Release Delivery System. <https://doi.org/10.1021/acs.molpharmaceut.9b00344>.
- Shah, S.S., Cha, Y., Pitt, C.G., 1992. Poly (glycolic acid-co-dl-lactic acid): diffusion or degradation controlled drug delivery? *J. Control. Release* 18 (3), 261–270. [https://doi.org/10.1016/0168-3659\(92\)90171-M](https://doi.org/10.1016/0168-3659(92)90171-M).
- Siepmann, J., Elkharraz, K., Siepmann, F., Klose, D., 2005. How autocatalysis accelerates drug release from PLGA-based microparticles: a quantitative treatment. *Biomacromolecules* 6 (4), 2312–2319. <https://doi.org/10.1021/bm050228k>.
- Sun, Y., Jensen, H., Petersen, N.J., Larsen, S.W., Østergaard, J., 2017. Phase separation of in situ forming poly (lactide-co-glycolide acid) implants investigated using a hydrogel-based subcutaneous tissue surrogate and UV-vis imaging. *J. Pharm. Biomed. Anal.* 145, 682–691. <https://doi.org/10.1016/j.jpba.2017.07.056>.
- Sun, F., Sun, X., Wang, H., Li, C., Zhao, Y., Tian, J., Lin, Y., 2022. Application of 3D-Printed, PLGA-Based Scaffolds in Bone Tissue Engineering. *Int. J. Mol. Sci.* 23, 1–15. <https://doi.org/10.3390/ijms23105831>.
- Takahashi, M., Onishi, H., Machida, Y., 2004. Development of implant tablet for a week-long sustained release, 100, 63–74. <https://doi.org/10.1016/j.jconrel.2004.07.031>.
- Tamani, F., Bassand, C., Hamoudi, M.C., Danede, F., Willart, J.F., Siepmann, F., Siepmann, J., 2019. Mechanistic explanation of the (up to) 3 release phases of PLGA microparticles: Diprophylline dispersions. *Int. J. Pharm.* 572 (August), 118819 <https://doi.org/10.1016/j.ijpharm.2019.118819>.
- Tamani, F., Bassand, C., Hamoudi, M.C., Siepmann, F., Siepmann, J., 2021. Mechanistic explanation of the (up to) 3 release phases of PLGA microparticles: Monolithic dispersions studied at lower temperatures. *Int. J. Pharm.* 596 (December 2020) <https://doi.org/10.1016/j.ijpharm.2021.120220>.
- Wan, F., Yang, M., 2016. Design of PLGA-based depot delivery systems for biopharmaceuticals prepared by spray drying. *Int. J. Pharm.* 498 (1–2), 82–95. <https://doi.org/10.1016/j.ijpharm.2015.12.025>.
- Wang, B., Wang, J., Shao, J., Kouwer, P.H.J., Bronkhorst, E.M., Jansen, J.A., Walboomers, X.F., Yang, F., 2020. A tunable and injectable local drug delivery system for personalized periodontal application. *J. Control. Release* 324 (April), 134–145. <https://doi.org/10.1016/j.jconrel.2020.05.004>.
- Ye, F., Larsen, S.W., Yagmur, A., Jensen, H., Larsen, C., Østergaard, J., 2012. Drug release into hydrogel-based subcutaneous surrogates studied by UV imaging. *J. Pharm. Biomed. Anal.* 71, 27–34. <https://doi.org/10.1016/j.jpba.2012.07.024>.
- Yelles, M.C.H., Tan, V.T., Danede, F., Willart, J.F., Siepmann, J., 2017. PLGA implants : how Poloxamer / PEO addition slows down or accelerates polymer degradation and drug release. *J. Control. Release* 253, 19–29. <https://doi.org/10.1016/j.jconrel.2017.03.009>.
- Zhong, H., Chan, G., Hu, Y., Hu, H., Ouyang, D., 2018. A comprehensive map of FDA-approved pharmaceutical products. *Pharmaceutics* 10 (4), 1–19. <https://doi.org/10.3390/pharmaceutics10040263>.